



Cite this: DOI: 10.1039/d6sc01540a

All publication charges for this article have been paid for by the Royal Society of Chemistry

Received 23rd February 2026
Accepted 4th May 2026

DOI: 10.1039/d6sc01540a

rs.c.li/chemical-science

Air-tolerant solar reforming of pre-treated biomass and plastics in viscous sustainable solvents

Dongseok Kim, Papa K. Kwarteng  and Erwin Reisner *

We report an air-tolerant solar reforming (SR) system for the valorisation of pre-treated biomass and plastic waste streams. This process operates in low O₂-diffusivity solvents such as the robust deep eutectic solvent (DES) ZnCl₂-acetamide, which prevents O₂ from interfering with photocatalysis by avoiding easily oxidisable components (e.g. alcohols) in water. This approach sustains SR performance under aerobic conditions using a carbon nitride photocatalyst, enabling photooxidative valorisation of depolymerised cellulose and polyethylene terephthalate (PET) while generating H₂ fuel. SR using low O₂-diffusivity solvents is scalable and also adaptable to non-innocent viscous liquid wastes such as glycerol, which can act as both the low O₂-diffusivity solvent to exclude O₂ and the organic waste source to produce valuable chemicals.

Introduction

Photocatalytic H₂ production using solar energy is a promising strategy to produce sustainable fuel as an alternative to conventional carbon-intensive H₂ production methods.^{1,2} While overall water splitting offers a pathway for clean H₂ production, its practical implementation has been hampered by its highly endothermic reaction and co-evolution of O₂ with limited commercial value.³ Solar reforming (SR) employs waste streams such as biomass or synthetic polymers (plastics) as electron donors, thereby lowering the energy barrier of the reaction, enhancing value creation by co-producing organic chemicals from waste oxidation without O₂ evolution and thus improving commercial prospects.^{4,5}

The production of H₂ through SR has therefore received significant attention, but the process requires anaerobic conditions as O₂ (air) is known to have a detrimental effect on photocatalytic performance. (Photo)catalytic H₂-evolution systems perform generally poorly in the presence of O₂ due to the thermodynamically favourable O₂ reduction reaction to produce reactive oxygen species (ROS) unless specific protection mechanisms are in place.⁶ Thus, inert atmospheres such as N₂ or Ar are commonly employed in photo(electro)catalytic H₂ production. However, tolerance to air is practically important as some exposure will be unavoidable in commercial or industrial deployment.⁷ While the development of O₂-tolerant solid-state,⁸ metal complex,^{9,10} and enzymatic H₂ catalysts^{11,12} is an active area of research, it remains unexplored in SR.

Deep eutectic solvents (DESs) have emerged as a novel class of green solvents characterised by their ease of preparation, low cost, and recyclability as well as their tuneable physicochemical

properties (e.g., negligible vapour pressure), and environmental friendliness (e.g., biodegradability).^{13,14} DESs are typically formed through the complexation of a hydrogen bond donor and a hydrogen bond acceptor, often involving readily available components such as choline chloride and urea. DESs exhibit melting points significantly lower than those of their individual constituents due to strong hydrogen bonding interactions. Their unique solvent properties have enabled widespread applications across diverse fields, including catalysis,^{15,16} electrochemistry,^{17,18} and materials synthesis,¹⁹ thereby positioning DESs as versatile media for green and sustainable chemistry.

It has recently been demonstrated that O₂-sensitive methyl viologen radicals can be stably generated *via* electrochemical, chemical, and photochemical methods and retained in DESs under air.²⁰ This ultrastability is attributed to the significantly reduced O₂ diffusivity in DESs, which protects the radicals from oxidative degradation under aerobic conditions. Low O₂-diffusivity also led to the development of air-tolerant redox flow batteries by using pyridinium-based electrolytes, effectively mitigating capacity fade caused by reduced radical species.²¹ These findings highlight the possibilities of developing air-tolerant solvent systems with potential impact across various applications. Various DESs have also been used to demonstrate O₂-tolerant H₂ production,^{22,23} and CO₂ reduction,²⁴ but these photocatalytic systems required easily-oxidisable sacrificial electron donors (e.g., triethanolamine) as the DESs contained primary alcohols which can be readily oxidised and thereby decomposed under photocatalytic conditions. To extend this strategy for practical depolymerisation in SR processes, robust SR systems with DESs resistant to oxidative decomposition during the photocatalytic cycle are required.

Here, we report a DES, composed of ZnCl₂ and acetamide (denoted as ZnAce), which is suitable for aerobic SR of polymeric waste streams. ZnAce, which avoids the presence of easily

Yusuf Hamied Department of Chemistry, University of Cambridge, Lensfield Road, Cambridge, CB2 1EW, UK. E-mail: reisner@ch.cam.ac.uk



oxidisable primary alcohols commonly present in widely used DESs, exhibits high stability during SR cycles and thereby enables the selective, challenging oxidation of waste substrates without undergoing oxidation itself. SR in aqueous ZnAce thereby facilitates air-tolerant SR of pre-treated biomass and plastics to produce H₂, maintaining SR performance under air without a significant loss in activity (Scheme 1). We further show that aerobic SR can be readily scaled up. Air-tolerant SR can even be achieved under practical conditions using viscous liquid waste streams such as glycerol and ethylene glycol, which act directly as the low O₂-diffusivity solvent and organic substrate without DES. Our approach thus offers a versatile and scalable platform for aerobic operation of SR in the future.

Results and discussions

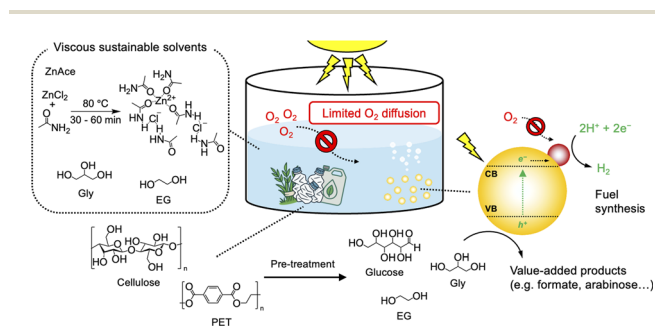
Cyanamide-functionalised carbon nitride modified with a platinum H₂ evolution co-catalyst was prepared and characterised as previously reported,^{25,26} and used as a photocatalyst in this study (see experimental Section, Fig. S1). The platinum co-catalyst also displays a well-established activity in catalysing the O₂ reduction reaction, which helps to investigate the performance of ZnAce in promoting O₂-tolerance of the dispersed photocatalyst solution when exposed to aerobic conditions. ZnAce was prepared following a previously reported procedure by stirring a mixture of ZnCl₂ and acetamide (1 : 4 molar ratio) at 80 °C until a homogeneous liquid was formed.²⁷

SR was optimised in the robust DES, ZnAce, which is free of readily oxidisable primary alcohols typical of many DESs, and carried out in a glass reactor with full solar spectrum irradiation (100 mW cm⁻², AM 1.5G) at 25 °C in a 3 mL solution of ZnAce with an aqueous solution containing glucose (50 mg mL⁻¹, ~280 mM) and phosphate buffer (KP_i, 10 mM, pH 4.5). Mildly acidic conditions were selected because the aqueous ZnAce solution precipitated under alkaline conditions (pH ≥ 7), most likely due to disruption of the ionic interactions between ZnCl₂ and acetamide (Fig. S2). Glucose is the soluble monomeric building block of cellulose and was therefore selected as a model electron donor. The glass reactor was charged with a solution containing the platinised carbon nitride (5 mg, Pt-loading 0.60 ± 0.03 wt%), sealed with a rubber septum to

collect the produced H₂, and the headspace contained air for aerobic SR or N₂ containing 2% CH₄ as an internal standard for anaerobic SR. The produced H₂ was periodically monitored by analysing the headspace (4.8 mL) of the photoreactor using gas chromatography.

To investigate the effect of ZnAce on H₂ production, the SR performance was initially screened under N₂ by varying the reaction medium composition between ZnAce and the KP_i buffered aqueous solution (Fig. 1a and S3). The activities under N₂ gradually increased with the addition of water due to the improved supply of protons. However, a different trend was observed under air, where adverse effects on photocatalysis emerged above 60% of H₂O_{KP_i} contents with negligible H₂ production in pure aqueous solution (see below for details). Importantly, the SR performance under air was nearly comparable with the N₂ purged system up to 40% of H₂O_{KP_i} content, with a maximal activity of 1610 ± 114 μmol H₂ per g_{CN_x} (53.7 ± 3.80 μmol H₂ per g_{substrate}) under N₂ and 1620 ± 143 μmol H₂ per g_{CN_x} (54.0 ± 4.78 μmol H₂ per g_{substrate}) under air after 18 h of SR in ZnAce : H₂O_{KP_i} (6 : 4 v/v) solution (see Table S1 for literature comparison). The marginal differences in SR performance under N₂ and air implied that atmospheric O₂ did not significantly hamper the catalytic cycle of the photocatalyst in ZnAce.

Exclusion control experiments in air and N₂ showed no or negligible amounts of H₂ in the absence of electron donor, co-catalyst or light, verifying that ZnAce was not involved in the SR process (Table 1).



Scheme 1 Schematic illustration of air-tolerant SR of pre-treated cellulose and PET with a platinised carbon nitride photocatalyst using viscous sustainable solvents such as ZnAce, glycerol (Gly), or ethylene glycol (EG).

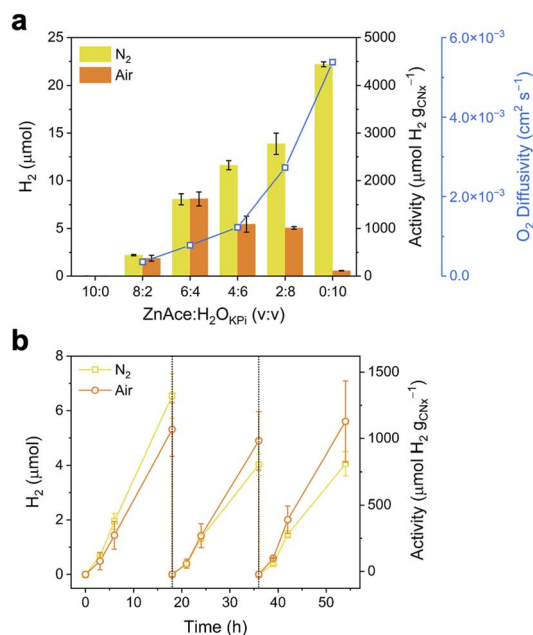


Fig. 1 SR performance under N₂ or air using a platinised carbon nitride photocatalyst with glucose (50 mg mL⁻¹) as an electron donor in ZnAce : H₂O_{KP_i} (H₂O contains 10 mM KP_i at pH 4.5) under simulated solar light irradiation (100 mW cm⁻², AM 1.5G) at 25 °C. (a) H₂ generation after 18 h and O₂-diffusivity as a function of the ZnAce : H₂O_{KP_i} ratio. (b) Glucose SR performance with photocatalyst recycling every 18 h, where the supernatant was removed and fresh ZnAce:H₂O_{KP_i} (6 : 4 v/v) solution and substrate added.



A comparison experiment was executed to identify the oxidative stability of different types of DESs under the oxidatively demanding conditions of SR using the photocatalyst. The most widely used DESs contain easily oxidisable alcohols (reline: choline chloride and urea; ethaline: choline chloride and ethylene glycol; glyceline: choline chloride and glycerol; Fig. S4), and a significant amount of H₂ was detected during irradiation even in the absence of an external electron donor, indicating that these DESs oxidatively decompose and are not suitable for SR (Fig. S5). This is supported by linear sweep voltammograms (LSV) of DES : H₂O_{KP_i} (6 : 4 v/v) solutions under N₂, which demonstrate that ZnAce is more stable under oxidative conditions (anodic potential) compared to other DESs (Fig. S6). These results highlight that ZnAce provides a uniquely robust medium for air-tolerant SR of waste streams in the aqueous DES.

Molybdenum disulfide (MoS₂) was also employed as co-catalyst instead of the precious-metal Pt for SR of glucose, and exhibited similar behaviour to Pt without significant decrease in performance under air compared to N₂ (Fig. S7).

To elucidate the origin of the air-tolerant SR, several physicochemical properties of the ZnAce : H₂O_{KP_i} solutions, O₂ solubility, viscosity, and O₂ diffusivity, were systematically investigated. As summarised in Table 2 and Fig. S8, increasing the ZnAce content led to a noticeable rise in viscosity, accompanied by an increase in O₂ solubility. Notably, the O₂ diffusivity calculated from the Levich equation (see experimental Section in SI for details) decreased as the ZnAce concentration increased, suggesting that suppressed O₂ mass transport is a key factor enabling air-tolerant SR (Fig. 1a). This observation is consistent with the Stokes–Einstein relationship, where higher solution viscosity results in reduced molecular diffusion. Accordingly, the increased viscosity of the ZnAce : H₂O_{KP_i} solution restricts O₂ diffusion, thereby limiting the oxygen reduction reaction (ORR) kinetics and effectively facilitating SR under aerobic conditions. At the same time, however, viscosity is also closely associated with proton diffusion; consequently, the H₂ production activity decreases as viscosity increases. These opposing effects reveal an inherent trade-off between minimising ORR and maintaining efficient H₂ production. On the basis of this balance, the optimal reaction condition was identified as a 6 : 4 volume ratio of ZnAce : H₂O_{KP_i}.

To directly validate the limited ORR during SR, O₂ levels were monitored in the headspace to confirm O₂ consumption during

glucose SR (Fig. S9). O₂ reduction is competing with proton reduction and occurs substantially in pure H₂O, causing 48% of O₂ consumption (~21.5 μmol, which is comparable to the amount of generated H₂ from SR under N₂) after 24 h. In contrast, only 7.0% of O₂ was consumed in the headspace above the ZnAce : H₂O_{KP_i} (6 : 4 v/v) solution. These data support that O₂ cannot effectively diffuse in the aqueous ZnAce medium, and the solvent thereby protects the photocatalyst from O₂ exposure, thereby enabling efficient photocatalytic H₂ production under aerobic conditions.

The oxidation products were determined by high-performance liquid chromatograph (HPLC) and ¹H nuclear magnetic resonance (NMR) spectroscopy after SR of glucose with the platinised carbon nitride photocatalyst in ZnAce : H₂O (6 : 4 v/v) mixture (Fig. S10). The main products of glucose SR in ZnAce/H₂O_{KP_i} were arabinose (C₅H₁₀O₅) and formate (HCOO⁻), which is consistent with the results of SR in H₂O under N₂.²⁸ Although the quantified oxidation products were not stoichiometrically matched with the reduced products (*ca.* 2 : 1 Red : Ox), we speculate that formate may undergo further oxidation to CO₂,²⁹ which could account for the observed stoichiometry. Importantly, the formation of arabinose and formate indicates that ZnAce does not alter the reaction selectivity or directly participates in the photocatalytic SR cycle, but instead primarily regulates O₂ diffusion, thereby enabling air-tolerant SR.

The platinised carbon nitride photocatalyst could be retrieved through centrifugation and reused by re-suspending in a fresh ZnAce : H₂O_{KP_i} solution, followed by glucose SR under simulated solar light. The recycled photocatalyst maintained over 60% of its activity under N₂ and nearly 100% under air of its SR activity compared to the previous 18 h irradiation interval (Fig. 1b). To further assess the robustness of the photocatalyst in the aqueous ZnAce medium, a 5 day continuous stability test was performed under the simulated solar light irradiation (Fig. S11). No noticeable decline in the H₂ production rate was observed throughout the extended SR operation, demonstrating the sustained stability of the air-tolerant SR system.

X-ray Photoelectron Spectroscopy (XPS) and Inductively Coupled Plasma Optical Emission Spectroscopy (ICP-OES) of the photocatalyst, following washing and drying after 18 h of SR, revealed some photo-deposition of Zn⁰ and surface adsorption of Zn²⁺ ions on the carbon nitride (Fig. S12). In addition, transmission electron microscopy coupled with

Table 1 Exclusion control experiments for SR of glucose (50 mg mL⁻¹) in ZnAce : H₂O_{KP_i} (6 : 4 v/v; H₂O contains 10 mM KP_i at pH 4.5) under N₂ or air using a platinised carbon nitride photocatalyst under simulated solar light irradiation (100 mW cm⁻², AM 1.5G) at 25 °C after 18 h. Blank (–) means the number of produced gases was less than the limit of detection (0.01 μmol)

	N ₂			Air		
	H ₂ [μmol]	Activity [μmol H ₂ per g _{CN_s}]	Yield [μmol H ₂ per g _{Substrate}]	H ₂ [μmol]	Activity [μmol H ₂ per g _{CN_s}]	Yield [μmol H ₂ per g _{Substrate}]
Full system	8.05 ± 0.57	1610 ± 114	53.7 ± 3.80	8.09 ± 0.72	1620 ± 143	54.0 ± 4.8
No SED	0.04 ± 0.00	8.89 ± 0.06	0.30 ± 0.01	0.031 ± 0.01	6.18 ± 2.00	0.21 ± 0.07
No Pt	0.05 ± 0.01	10.3 ± 1.25	0.34 ± 0.04	0.04 ± 0.01	7.89 ± 0.91	0.26 ± 0.03
No light	–	–	–	–	–	–



Table 2 Kinematic viscosities and O₂ diffusivities at 1 atm air and O₂ solubilities under O₂ saturated conditions in the ZnAce : H₂O_{KP} solutions

ZnAce : H ₂ O _{KP} (v/v)	Kinematic viscosity (cm ² s ⁻¹)	O ₂ solubility (mmol L ⁻¹)	O ₂ diffusivity (cm ² s ⁻¹)
0 : 10	1.07 ± 0.032 × 10 ⁻²	0.121 ± 0.047	5.38 × 10 ⁻³
2 : 8	2.88 ± 0.040 × 10 ⁻²	0.222 ± 0.036	2.73 × 10 ⁻³
4 : 6	4.84 ± 0.104 × 10 ⁻²	0.361 ± 0.040	1.23 × 10 ⁻³
6 : 4	6.59 ± 0.040 × 10 ⁻²	0.469 ± 0.040	7.78 × 10 ⁻⁴
8 : 2	8.53 ± 0.040 × 10 ⁻²	0.653 ± 0.045	3.58 × 10 ⁻⁴

energy-dispersive X-ray (TEM-EDX) analysis also confirmed the presence of Zn on the catalyst surface, but no significant structural damage or detrimental changes to the photocatalyst were observed (Fig. S13). Despite the unexpected Zn-deposit on the photocatalyst, the retained recyclability under air, structural integrity, and long-term stability of the photocatalyst indicated that ZnAce did not exert a detrimental influence on SR performance and catalyst recyclability.

Air-tolerant SR (100 mg of substrates) into H₂ using a ZnAce : H₂O_{KP} (6 : 4 v/v) mixture was subsequently studied using polymeric substrates, *viz.* cellulose and xylan, along with their soluble substrates (Fig. 2a).³⁰ As the solubility of the substrates in ZnAce/H₂O_{KP} increases, improved photocatalyst-substrate contact leads to significantly enhanced SR activity. After 18 h of simulated solar light irradiation, xylose produced 1010 ± 92 μmol H₂ per g_{CN_x} under N₂ and 677 ± 127 μmol H₂ per g_{CN_x} under air, and galactose generated 932 ± 112 μmol H₂ per g_{CN_x} under N₂ and 860 ± 202 μmol H₂ per g_{CN_x} under air. The SR performance for insoluble, polymeric α-cellulose and xylan was 59.6 ± 20.7 μmol H₂ per g_{CN_x} under N₂ and 27.6 ± 4.43 μmol H₂ per g_{CN_x} under air, and 141 ± 39.2 μmol H₂ per g_{CN_x} under N₂ and 105 ± 36.8 μmol H₂ per g_{CN_x} under air, respectively. These results showed that the air-tolerant SR system could be successfully extended to various biomass substrates.

Further expansion to air-tolerant SR of polymer waste using ZnAce : H₂O_{KP} was conducted by utilising ethylene glycol (EG), a monomeric component of polyethylene terephthalate (PET), as a substrate.³¹ H₂ production coupled with EG oxidation exhibited significant activity of 805 ± 58 μmol H₂ per g_{CN_x} under N₂ and 769 ± 37 μmol H₂ per g_{CN_x} under air after 18 h in a ZnAce : H₂O_{KP} (6 : 4 v/v) solution (Fig. 2a). Thus, the SR activity of the PET monomer EG was retained under air compared to inert conditions.

In addition, glycerol (Gly), an industrially relevant alcohol and major byproduct of biodiesel, was also used as a substrate for air-tolerant SR (Fig. 2a).³² The SR of Gly in ZnAce : H₂O_{KP} showed slightly lower performance under air, but it still achieved a notable value of 513 ± 79.9 μmol H₂ per g_{CN_x}, considering that the reaction was performed in the presence of O₂.

Subsequently, insoluble and robust polymeric substrates such as cellulose, xylan, and PET were subjected to acid hydrolysis pre-treatment using an aqueous H₂SO₄ solution at 120–140 °C depending on the substrate (see experimental Section in SI for details) to more completely depolymerise them into soluble monomers, glucose, xylose, and EG (72% conversion yield for PET according to a previous report; Fig. 2b).^{33,34} The pre-treated solutions were then diluted 10 times and directly used for SR. This pre-treatment step ensures suitable

reaction kinetics and better accessibility of monomers to the photocatalyst for SR. It significantly improved the SR performances, yielding activities of 445 ± 41.5 μmol H₂ per g_{CN_x} for cellulose, 545 ± 127 μmol H₂ per g_{CN_x} for xylan, and 388 ± 29.1 μmol H₂ per g_{CN_x} for PET, respectively, after 18 h of SR in ZnAce : H₂O_{acid} (6 : 4 v/v) solution under air.

Intriguingly, the SR performance for cellulose under air was higher than under N₂, which is likely due to the generation of ROS *via* residual ORR in the reaction mixture, promoting subsequent fragmentation of partially degraded cellulose into smaller, more readily oxidisable intermediates and thereby enhancing the overall SR efficiency. A control experiment was

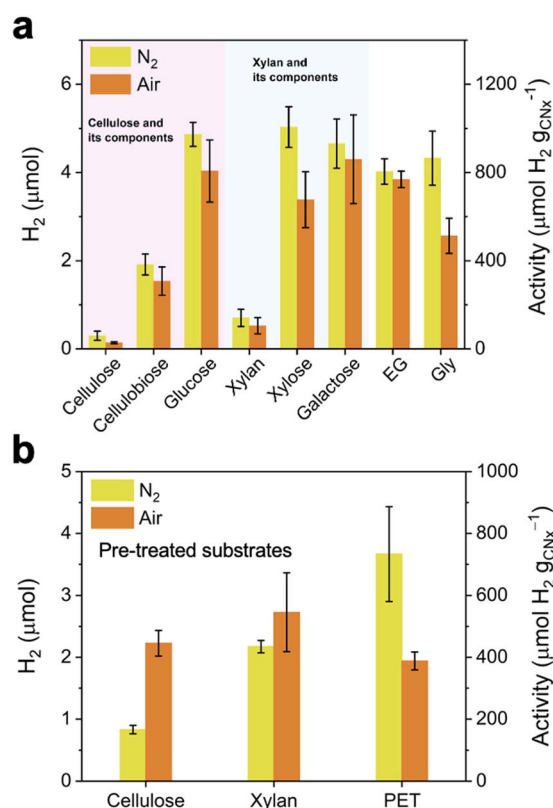


Fig. 2 (a) SR performance coupled with H₂ production after 18 h under N₂ or air using platinumised carbon nitride photocatalyst in 3 mL of ZnAce : H₂O_{KP} (10 mM, pH 4.5) in H₂O (6 : 4 v/v) for lignocellulosic components, EG, and Gly (100 mg). (b) SR performance after 18 h under N₂ or air using pre-treated cellulose, xylan and PET in 3 mL of ZnAce : 0.75 M H₂SO₄ (6 : 4 v/v) solution under N₂ and air. All experiments were conducted under simulated solar light irradiation (100 mW cm⁻², AM 1.5G) at 25 °C.



carried out using the radical scavenger 5,5-dimethyl-1-pyrroline *N*-oxide (DMPO) (Fig. S14). The presence of the radical scavenger showed no significant difference between N_2 and air, supporting the speculation that the higher SR activity for cellulose under aerobic conditions in ZnAce : H_2O_{acid} (6 : 4 v/v) solution is mainly attributed to ROS-mediated fragmentation of cellulose into oxidisable species, despite the anticipated low ROS levels resulting from inhibited ORR in the aqueous ZnAce solution. Nevertheless, additional mechanistic investigation will be required in future studies to fully understand the increased aerobic SR activity.

Next, the scalability of the air-tolerant SR system was demonstrated to simulate real-world conditions more closely. The scale-up employed a large polyethylene reactor (0.02 m² irradiation area, 1.7 L reactor volume) with a borosilicate glass window allowing vertical irradiation of a 300 mL SR solution (Fig. 3a).³⁴ The same reaction conditions used for the smaller scale aerobic SR were employed, including the concentration of catalyst and substrate as well as the ZnAce/ H_2O_{KPI} solution composition. Using an LED array as the light source (400 nm, 8 mW cm⁻²), the large-scale air-tolerant SR produced 3.68 mmol \pm 0.82 of H_2 (7.35 \pm 1.63 mmol H_2 per g_{CN_x} , 36.8 \pm 8.15 μ mol H_2 per g_{CN_x} cm⁻²) from EG oxidation with an apparent quantum yield (AQY) of 0.52%, and 1.42 mmol \pm 0.29 of H_2 (2.83 \pm 0.589 mmol H_2 per g_{CN_x} , 14.2 \pm 2.95 μ mol H_2 per g_{CN_x} cm⁻²) from glucose SR with an AQY of 0.20% under air after 72 h (Fig. 3b), showing that

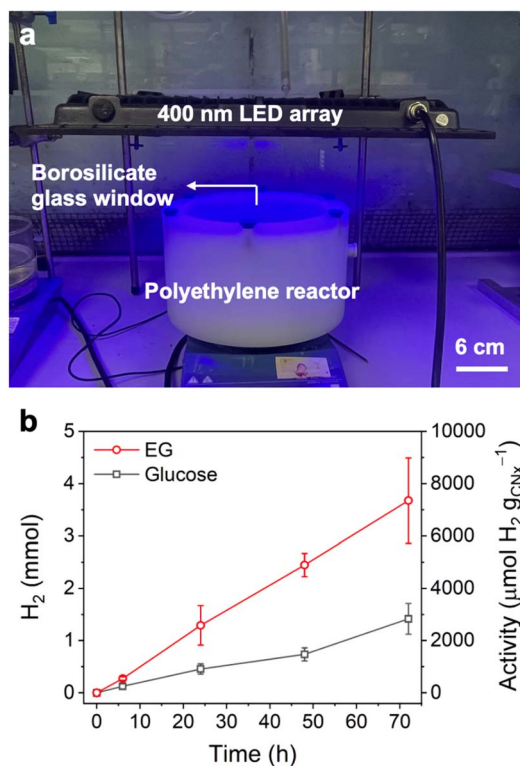


Fig. 3 (a) Image of the large-scale setup and (b) H_2 production using platinumised carbon nitride photocatalyst coupled with glucose and ethylene glycol oxidation through upscaled SR under air ($V_{total} = 300$ mL), performed under 400 nm LED irradiation (8 mW cm⁻²); all concentrations were kept constant.

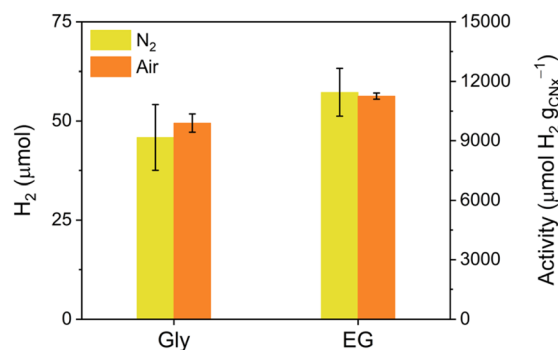


Fig. 4 SR performance after 18 h under N_2 and air using platinumised carbon nitride photocatalyst in 3 mL of viscous liquid wastes : H_2O_{KPI} (10 mM, pH 4.5) in H_2O (6 : 4 v/v) solution under simulated solar light irradiation (100 mW cm⁻², AM 1.5G) at 25 °C.

this cost-effective and simple air-tolerant SR system could be successfully applied to large-scale operation.

Given that the high viscosity of the DES reaction medium leads to reduced O_2 diffusivity and thereby enables the air-tolerant SR, we investigated the feasibility of employing viscous liquid waste directly as a substitute for the DES in order to broaden the applicability of the air-tolerant SR system. In other words, the viscous liquid waste can act directly as both the O_2 -protected reaction medium and the electron donor for SR instead of using ZnAce plus an additional solubilised waste substrate. Accordingly, Gly and EG were subjected to air-tolerant SR using glycerol : H_2O_{KPI} (6 : 4 v/v) and EG : H_2O_{KPI} (6 : 4 v/v) solutions, respectively (Fig. 4). In these air-tolerant SR systems, exceptional SR performance was achieved, exhibiting 9670 \pm 1660 μ mol H_2 per g_{CN_x} under N_2 and 9890 \pm 460 μ mol H_2 per g_{CN_x} under air for Gly, and 11 400 \pm 1200 μ mol H_2 per g_{CN_x} under N_2 and 11 300 \pm 158 μ mol H_2 per g_{CN_x} under air for EG. Hence, the viscous liquid wastes provided the electron donor for SR in very high concentration and also limited O_2 diffusivity in the reaction mixture, thereby enabling efficient air-tolerant SR (Table S2). Moreover, Levich plot analysis based on the rotating disk electrode (RDE) voltammetry under O_2 -saturated conditions showed that the introduction of viscous liquids (ZnAce, EG, and Gly) effectively suppressed O_2 mass transport rate with lowering ORR activity, resulting in sustained photocatalytic SR under aerobic conditions (Fig. S15, S16, Tables S3 and S4).

Beyond monomeric alcoholic waste substrates, polymeric viscous liquid wastes such as polypropylene glycol, polyethylene glycol, and honey were also tested as a reaction medium (Fig. S17). Although the SR activity was relatively low, likely due to the large and complex matrix of the substrate, air-tolerant SR was still achievable with direct use of the polymeric liquid wastes. As a control, methanol, a low-viscosity alcohol, was tested and showed negligible SR performance under air, confirming that high-viscosity liquids are critical to achieve air-tolerant SR.

Conclusions

We have established an air-tolerant and practical SR system by adjusting the reaction medium to a high viscosity, low O_2 -



diffusivity solvent mixed with water. We have identified ZnAce as a robust DES that enables photocatalytic valorisation of pre-treated biomass and plastics, while preventing O₂ interference with oxidation of organics in solution and simultaneously enabling H₂ fuel production under air. This SR system maintains its photocatalytic performance under aerobic conditions without significant loss because O₂ cannot effectively reach the photocatalyst due to the limited mass transport of O₂ in the viscous solvent mixture. This solvent mixture facilitates a mechanism proceeding *via* direct hole transfer from the photocatalyst to the substrate, resulting in the same oxidation products as those observed in established SR systems operating in aqueous solutions under N₂. This air-tolerant SR system was applied to the conversion of insoluble polymeric lignocellulosic biomass (*e.g.*, xylan, cellulose) and plastic waste (*e.g.*, PET), where the SR performance can be substantially enhanced by employing acid pre-treatment to break the bulky substrates into soluble organic feedstocks. The scalability of the air-tolerant SR system was validated through scaled-up demonstrations of SR using waste substrates. Notably, the SR system also accommodated viscous liquid waste instead of DES to be used as electron donor and to promote O₂-tolerance, underscoring its adaptability and versatility. This simple and robust strategy for achieving air-tolerant SR holds potential for practical deployment in biomass and plastic waste treatment with sustainable fuel generation. In the future, low O₂-diffusivity solvents may also pave the way for air-tolerant organic photocatalysis.

Author contributions

D. K. and E. R. designed the project. D. K. conducted the main experimental work, including photocatalyst synthesis and characterisation, photocatalysis, product quantification and characterisation, electrochemical analysis, and data analysis. P. K. K. designed the large-scale reactor and conducted acid pre-treatment. D. K. and E. R. co-wrote the manuscript with contributions from P. K. K.

Conflicts of interest

A patent application covering this work has been filed by Cambridge Enterprise that names all co-authors as inventors (GB2518549.7; 06. Nov. 2025).

Data availability

The data that support the findings of this study are openly available at the Cambridge Data repository: <https://doi.org/10.17863/CAM.130162>.

Supplementary information (SI) is available. See DOI: <https://doi.org/10.1039/d6sc01540a>.

Acknowledgements

We acknowledge support from the UK Department of Science, Innovation & Technology and the Royal Academy of Engineering

Chair in Emerging Technologies programme (CIET-2324-83), UKRI for an ERC Advanced Grant (EP/X030563/1), the Yusuf Hamied Department of Chemistry, and the Cambridge Trust. Dr Virgil Andrei is acknowledged for assistance with the quantification of oxygen gas, and Dr Shannon Bonke and Dr Chan Woo Lee for helpful feedback and discussions.

References

- 1 J. Goldemberg, *Science*, 2007, **315**, 808–810.
- 2 T. R. Cook, D. K. Dogutan, S. Y. Reece, Y. Surendranath, T. S. Teets and D. G. Nocera, *Chem. Rev.*, 2010, **110**, 6474–6502.
- 3 M. Park, M. Gu and B.-S. Kim, *ACS Nano*, 2020, **14**, 6812–6822.
- 4 S. Bhattacharjee, V. Andrei, C. Pornrungrroj, M. Rahaman, C. M. Pichler and E. Reisner, *Adv. Funct. Mater.*, 2022, **32**, 2109313.
- 5 D. S. Achilleos, W. Yang, H. Kasap, A. Savateev, Y. Markushyna, J. R. Durrant and E. Reisner, *Angew. Chem., Int. Ed.*, 2020, **59**, 18184–18188.
- 6 D. W. Wakerley and E. Reisner, *Energy Environ. Sci.*, 2015, **8**, 2283–2295.
- 7 T. Uekert, C. M. Pichler, T. Schubert and E. Reisner, *Nat. Sustain.*, 2021, **4**, 383–391.
- 8 K. Maeda, K. Teramura, D. Lu, N. Saito, Y. Inoue and K. Domen, *Angew. Chem., Int. Ed.*, 2006, **45**, 7806–7809.
- 9 W. T. Eckenhoff and R. Eisenberg, *Dalton Trans.*, 2012, **41**, 13004–13021.
- 10 F. Lakadamyali, M. Kato, N. M. Muresan and E. Reisner, *Angew. Chem., Int. Ed.*, 2012, **51**, 9381–9384.
- 11 T. Sakai, D. Mersch and E. Reisner, *Angew. Chem., Int. Ed.*, 2013, **52**, 12313–12316.
- 12 H. Li, D. Buesen, S. Dementin, C. Léger, V. Fourmond and N. Plumeré, *J. Am. Chem. Soc.*, 2019, **141**, 16734–16742.
- 13 E. L. Smith, A. P. Abbott and K. S. Ryder, *Chem. Rev.*, 2014, **114**, 11060–11082.
- 14 A. K. Halder and M. N. D. S. Cordeiro, *ACS Sustain. Chem. Eng.*, 2019, **7**, 10649–10660.
- 15 A. P. Abbott, T. J. Bell, S. Handa and B. Stoddart, *Green Chem.*, 2005, **7**, 705–707.
- 16 J. T. Gorke, F. Srienc and R. J. Kazlauskas, *Chem. Commun.*, 2008, 1235–1237.
- 17 C.-H. Liao, J.-Y. Chen, G.-Y. Liu, Z.-R. Xu, S. Lee, C.-K. Chiang and Y.-T. Hsieh, *ACS Omega*, 2022, **7**, 19930–19938.
- 18 C. Zhang, Y. Ding, L. Zhang, X. Wang, Y. Zhao, X. Zhang and G. Yu, *Angew. Chem., Int. Ed.*, 2017, **56**, 7454–7459.
- 19 H.-G. Liao, Y.-X. Jiang, Z.-Y. Zhou, S.-P. Chen and S.-G. Sun, *Angew. Chem., Int. Ed.*, 2008, **47**, 9100–9103.
- 20 J. A. McCune, M. F. Kuehnel, E. Reisner and O. A. Scherman, *Chem*, 2020, **6**, 1819–1830.
- 21 M. E. Carrington, K. Sokołowski, E. Jónsson, E. W. Zhao, A. M. Graf, I. Temprano, J. A. McCune, C. P. Grey and O. A. Scherman, *Nature*, 2023, **623**, 949–955.
- 22 M. G. Allan, M. J. McKee, F. Marken and M. F. Kuehnel, *Energy Environ. Sci.*, 2021, **14**, 5523–5529.



- 23 M. G. Allan, T. Pichon, J. A. McCune, C. Cavazza, A. Le Goff and M. F. Kühnel, *Angew. Chem., Int. Ed.*, 2023, **62**, e202219176.
- 24 J. Onodera, X. Zhang, T. Tanaka, R. Nakada, M. Okazaki, N. Tarutani, K. Katagiri and K. Maeda, *ACS Catal.*, 2026, **16**, 3368–3379.
- 25 J. Liu, Y. Liu, N. Liu, Y. Han, X. Zhang, H. Huang, Y. Lifshitz, S.-T. Lee, J. Zhong and Z. Kang, *Science*, 2015, **347**, 970–974.
- 26 H. Kasap, R. Godin, C. Jeay-Bizot, D. S. Achilleos, X. Fang, J. R. Durrant and E. Reisner, *ACS Catal.*, 2018, **8**, 6914–6926.
- 27 S. Hong, X. Sun, H. Lian, J. A. Pojman and J. D. Mota-Morales, *J. Appl. Polym. Sci.*, 2020, **137**, 48385.
- 28 E. Lam, M. Miller, S. Linley, R. R. Manuel, I. A. C. Pereira and E. Reisner, *Angew. Chem., Int. Ed.*, 2023, **62**, e202215894.
- 29 R. Muhammad Irfan, M. K. Zaman, M. H. Tahir, A. Ahmad, M. Tayyab, T. Ahmad, M. Hussain, I. Arshad and M. A. Shaheen, *ACS Appl. Energy Mater.*, 2023, **6**, 1834–1844.
- 30 H. Kasap, D. S. Achilleos, A. Huang and E. Reisner, *J. Am. Chem. Soc.*, 2018, **140**, 11604–11607.
- 31 T. Uekert, M. F. Kuehnel, D. W. Wakerley and E. Reisner, *Energy Environ. Sci.*, 2018, **11**, 2853–2857.
- 32 Y. Liu, B. Zhang, D. Yan and X. Xiang, *Green Chem.*, 2024, **26**, 2505–2524.
- 33 T. Yoshioka, T. Sato and A. Okuwaki, *J. Appl. Polym. Sci.*, 1994, **52**, 1353–1355.
- 34 P. K. Kwarteng, Y. Liu, C. Han, S. A. Bonke, D. M. Vahey, C. Pulignani and E. Reisner, *Joule*, 2026, **10**, 102347.

